

## Donor–acceptor nanoensembles of soluble carbon nanotubes†

Dirk M. Guldi,<sup>a,b</sup> G. N. A. Rahman,<sup>a</sup> Jeff Ramey,<sup>a</sup> Massimo Marcaccio,<sup>c</sup> Demis Paolucci,<sup>c</sup> Francesco Paolucci,<sup>\*c</sup> Shuhui Qin,<sup>d</sup> Warren T. Ford,<sup>\*d</sup> Domenico Balbinot,<sup>e</sup> Norbert Jux,<sup>\*e</sup> Nikos Tagmatarchis<sup>f</sup> and Maurizio Prato<sup>\*f</sup><sup>a</sup> Radiation Laboratory, University of Notre Dame, IN 46556, USA. E-mail: guldi.1@nd.edu<sup>b</sup> Institute for Physical Chemistry, Universität Erlangen-Nürnberg, 91058 Erlangen, Germany<sup>c</sup> Dipartimento di Chimica “G. Ciamician”, Università di Bologna, V. F. Selmi 2, 40126 Bologna, Italy. E-mail: francesco.paolucci@unibo.it<sup>d</sup> Department of Chemistry, Oklahoma State University, Stillwater, OK 74078, USA<sup>e</sup> Institut für Organische Chemie, Universität Erlangen-Nürnberg, 91054 Erlangen, Germany<sup>f</sup> Dipartimento di Scienze Farmaceutiche, Università di Trieste, Piazzale Europa 1, Trieste 34127, Italy. E-mail: prato@units.it

Received (in Cambridge, UK) 10th May 2004, Accepted 30th June 2004

First published as an Advance Article on the web 10th August 2004

Donor–acceptor nanoensembles, prepared via electrostatic interactions of single wall carbon nanotubes and porphyrin salts, give rise to photoinduced intra-complex charge separation that lasts tens of microseconds.

Single wall carbon nanotubes, SWNTs, are being considered for many applications, strong support coming from the increased knowledge of their properties.<sup>1,2</sup> The development of SWNT-based photovoltaic hybrids as potent alternatives to inorganic semi-conducting materials has, however, drawn much less attention.<sup>3</sup> Here we present the coulomb complex formation of a water-soluble SWNT grafted with poly(sodium 4-styrenesulfonate) (SWNT-PSS, Fig. 1) and an octapyridinium free base porphyrin salt  $H_2P^{8+}$  en route to versatile donor–acceptor ensembles and the proof for an intra-ensemble charge separation in SWNT-PSS<sup>n-</sup>/ $H_2P^{8+}$  that lives tens of microseconds.

SWNT-PSS, containing 55/45 SWNT/PSS by weight, was prepared by *in situ* free radical polymerization of sodium 4-styrenesulfonate in an aqueous dispersion of pristine HiPco SWNT.<sup>4</sup>

The cyclic voltammetric (CV) curve of a saturated SWNT-PSS<sup>n-</sup> aqueous solution, obtained in the negative potential region, displays a continuum of diffusion-controlled cathodic currents (Figure S1), with an onset at around  $-0.15$  V vs. SCE (Figure S2), which corresponds to the reduction of SWNT-PSS<sup>n-</sup>.<sup>5</sup> While the cathodic response was reproducible upon repetitive potential scanning up to  $-1.0$  V, oxidation at potentials  $>0.5$  V caused irreversible electrode fouling. Similarly to what was observed for pyrrolidine-functionalised NTs, this behavior is ascribed to the formation of a film on the electrode, through which electron transfer is hindered.

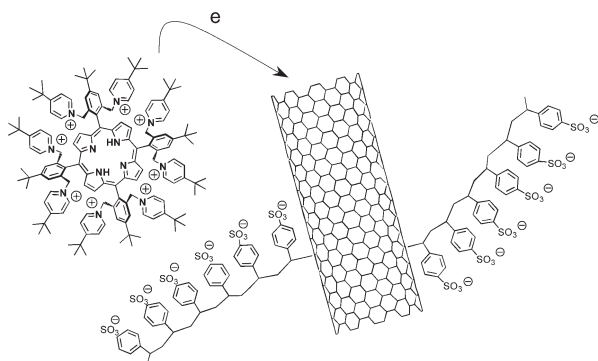


Fig. 1 Partial structure of SWNT-PSS<sup>n-</sup>/ $H_2P^{8+}$  used in this work.

† Electronic supplementary information (ESI) available: experimental data. See <http://www.rsc.org/suppdata/cc/b4/b406933a/>

First insight into the electrostatic binding of SWNT-PSS<sup>n-</sup> and  $H_2P^{8+}$  came from Transmission Electron Microscopy (TEM). One drop of dilute aqueous solution containing equivalent amounts of SWNT-PSS<sup>n-</sup> and  $H_2P^{8+}$  (0.1%) was cast onto a copper grid (3 mm, 200 mesh) coated with a formvar film. For SWNT-PSS<sup>n-</sup> thick bundles and ropes were evident, while for SWNT-PSS<sup>n-</sup>/ $H_2P^{8+}$  thinner bundles surrounded by dark areas were observed, most likely deriving from electrostatic interactions (Fig. 2).

The formation of SWNT-PSS<sup>n-</sup>/ $H_2P^{8+}$  was monitored by absorption and fluorescence techniques. A dilute aqueous solution of  $H_2P^{8+}$  ( $3.2 \times 10^{-6}$  M) was titrated with SWNT-PSS<sup>n-</sup>. Fig. 3 shows that a clean conversion from  $H_2P^{8+}$  to SWNT-PSS<sup>n-</sup>/ $H_2P^{8+}$  is observed through an isosbestic point at 424 nm, with red shift of the Soret- and Q-bands.

When SWNT-PSS<sup>n-</sup> was added to  $H_2P^{8+}$ , the fluorescence also underwent several key changes. Fig. 4 summarizes the steady-state fluorescence with 424 nm excitation. Firstly, the fluorescence intensities decrease exponentially and converge to a final plateau value. This trend is exemplified in the  $I/I_0$  versus SWNT-PSS<sup>n-</sup> concentration relationship, shown in the insert to Fig. 4. The

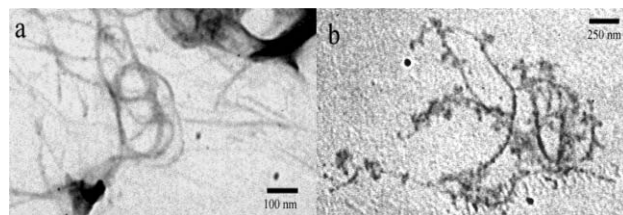


Fig. 2 TEM photos of (a) SWNT-PSS<sup>n-</sup> and (b) SWNT-PSS<sup>n-</sup>/ $H_2P^{8+}$ .

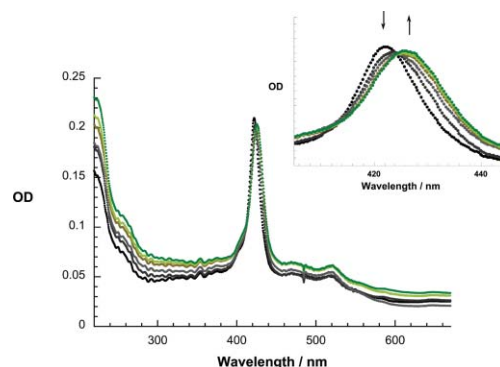
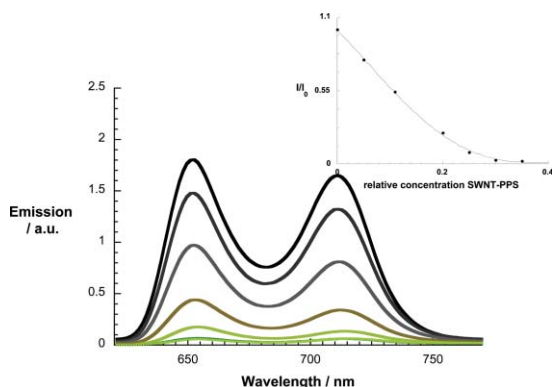


Fig. 3 Absorption spectra of a dilute aqueous solution of  $H_2P^{8+}$  ( $3.2 \times 10^{-6}$  M) upon adding SWNT-PSS<sup>n-</sup>. The inset zooms in on the 400–450 nm Soret-band region of  $H_2P^{8+}$ .



**Fig. 4** Fluorescence spectra of a dilute aqueous solution of  $\text{H}_2\text{P}^{8+}$  ( $3.2 \times 10^{-6}$  M) upon adding of SWNT-PSS $^{n-}$ —complementary to Fig. 3. Excitation is 424 nm. Insert:  $I/I_0$  versus SWNT-PSS $^{n-}$  relationship.

decrease in  $\text{H}_2\text{P}^{8+}$  fluorescence with SWNT-PSS $^{n-}$  is as large as 30 times. Secondly, the intensity of the fluorescence peaks at 651 and 711 nm shift progressively to the red with final maxima at 654 and 715 nm. This trend mirrors the changes in the ground state absorption spectra. Thirdly, the  $\text{H}_2\text{P}^{8+}$  fluorescence lifetime (*i.e.*, 10.2 ns), which in the absence of SWNT-PSS $^{n-}$  is best fitted by a mono-exponential rate law, is replaced by a bi-exponential decay. In the presence of SWNT-PSS $^{n-}$  a long- (10.2 ns) and a short-lived component (0.3 ns) are observed. The long-lived component relates to free  $\text{H}_2\text{P}^{8+}$  that is not associated with any SWNT-PSS $^{n-}$ , while the short-lived component is attributed to the deactivation within the SWNT-PSS $^{n-}/\text{H}_2\text{P}^{8+}$  nanoensemble. Finally, analyzing the pre-exponential factors of the two lifetime components, the long-lived one dominates only in the low SWNT-PSS $^{n-}$  concentration regime and, ultimately, disappears in the plateau region.<sup>6</sup>

Due to electrostatic attraction between the positively charged  $\text{H}_2\text{P}^{8+}$  and the polyanionic SWNT-PSS $^{n-}$ , stable SWNT-PSS $^{n-}/\text{H}_2\text{P}^{8+}$  ensembles are formed. The synopsis of the emission studies is a rapid singlet excited state deactivation *via* an intra-ensemble electron transfer. A thermodynamic correlation of the  $\text{H}_2\text{P}^{8+}$  singlet excited state (1.9 eV) with the radical ion pair state (1.09 eV:  $E_{\text{red}}$  (SWNT-PSS $^{n-}$ ) = -0.15 V;  $E_{\text{ox}}$  ( $\text{H}_2\text{P}^{8+}$ ) = +0.94 V vs. SCE<sup>7</sup>) further supports our postulate: charge separation is governed by a large  $-\Delta G_{\text{CS}}$  of 0.81 eV.

To corroborate that the electron transfer effects seen in SWNT-PSS $^{n-}/\text{H}_2\text{P}^{8+}$  are due to the presence of the SWNTs we also probed  $\text{H}_2\text{P}^{8+}$  with a commercial sample of PSS $^{n-}$ —see Figures S3 and S4. The absorption spectra still give rise to the trend summarized above for SWNT-PSS $^{n-}$ . However, no notable quenching was found in steady-state and time-resolved fluorescence experiments. This proves the electrostatically driven association of  $\text{H}_2\text{P}^{8+}$  with the negatively charged  $-\text{SO}_3^-$  head groups in either SWNT-PSS $^{n-}$  or PSS $^{n-}$ , but the lack of redox-activity of PSS $^{n-}$  alone prevents electron transfer deactivation of the fluorescence.

Spectroscopic evidence in support of a successful electron transfer quenching came from transient absorption measurements, following 532 nm laser excitation. The excitation wavelength guarantees the exclusive population of the  $\text{H}_2\text{P}^{8+}$  singlet excited states, which intersystem crosses with a time constant of 10 ns to the triplet manifold. The long-lived and molecular oxygen sensitive triplet spectrum is shown in Fig. 5. Besides bleaching in the Soret- and Q-band region, the most important characteristic is the triplet maximum at 775 nm.<sup>8</sup> The differential absorption changes of the SWNT-PSS $^{n-}/\text{H}_2\text{P}^{8+}$  ensemble, on the other hand, are governed by broad absorptions in the 550–800 nm range, indicating a  $\text{H}_2\text{P}^{8+}$  centered redox product.<sup>8</sup> The reduced form of SWNT-PSS $^{n-}$  has a

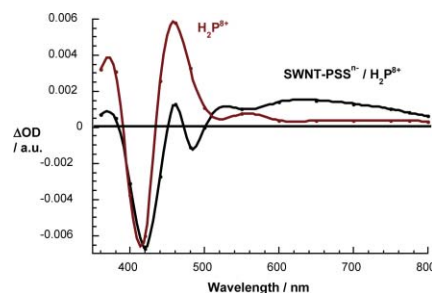


**Fig. 5** Differential absorption spectrum (visible and near-infrared) obtained upon nanosecond flash photolysis (532 nm) of  $\sim 1.2 \times 10^{-5}$  M solutions of  $\text{H}_2\text{P}^{8+}$  (red spectrum) and of SWNT-PSS $^{n-}/\text{H}_2\text{P}^{8+}$  (black spectrum) in nitrogen saturated solutions with a time delay of 100 ns.

broad maximum at 450 nm<sup>9</sup> that is masked by the strong changes associated with the redox chemistry of  $\text{H}_2\text{P}^{8+}$ .

Under anaerobic conditions, the lifetime of 14  $\mu\text{s}$  observed for the newly formed ion pair is remarkably long. The effect that molecular oxygen exerts on the lifetime of the ion pair state absorption is interesting. The lack of notable changes in the 550–800 nm region confirms that the  $\text{H}_2\text{P}^{8+}$  redox product must be the  $\pi$ -radical cation.<sup>10</sup> The transient absorption around 460 nm, on the other hand, shows decays that depend linearly on the oxygen concentration. This speaks for features of a reduced species (*i.e.*, SWNT-PSS $^{n-}$ ).

Part of this work was supported by the Office of Basic Energy Sciences of the U.S. Department of Energy (NDRL-4550 from the Notre Dame Radiation Laboratory), the Universities of Trieste and Bologna, the European Union (RTN program “WONDERFULL”), MIUR (PRIN 2002, prot. 2002032171), the National Science Foundation (EPS-0132543), and the Deutsche Forschungsgemeinschaft (SFB 583).

## Notes and references

- 1 Special issue of *Acc. Chem. Res.*, 2002, **35**, 997.
- 2 For recent reviews, see: (a) A. Hirsch, *Angew. Chem., Int. Ed.*, 2002, **35**, 1853; (b) J. L. Bahr and J. M. Tour, *J. Mater. Chem.*, 2002, **35**, 1952; (c) S. Niyogi, M. A. Hamon, H. Hu, B. Zhao, P. Bhomwik, R. Sen, M. E. Itkis and R. C. Haddon, *Acc. Chem. Res.*, 2002, **35**, 1105; (d) Y.-P. Sun, K. Fu, Y. Lin and W. Huang, *Acc. Chem. Res.*, 2002, **35**, 1096; (e) S. Banerjee, M. G. C. Kahn and S. S. Wang, *Chem. Eur. J.*, 2003, **35**, 1898; (f) D. Tasis, N. Tagmatarchis, V. Georgakilas and M. Prato, *Chem. Eur. J.*, 2003, **35**, 4000; N. Tagmatarchis and M. Prato, *J. Mater. Chem.*, 2004, **14**, 437.
- 3 D. M. Guldi, M. Marcaccio, D. Paolucci, F. Paolucci, N. Tagmatarchis, D. Tasis, E. Vázquez and M. Prato, *Angew. Chem., Int. Ed.*, 2003, **35**, 4206.
- 4 S. Qin, D. Qin, W. T. Ford, J. E. Herrera, D. E. Resasco, S. M. Bachilo and R. B. Weisman, *Macromolecules*, 2004, **35**, 3965.
- 5 An analogous CV behavior was found under aprotic conditions with soluble NTs functionalized by pyrrolidines: M. Melle-Franco, M. Marcaccio, D. Paolucci, F. Paolucci, V. Georgakilas, D. M. Guldi, M. Prato and F. Zerbetto, *J. Am. Chem. Soc.*, 2004, **35**, 1646.
- 6 The lifetime difference resembles quantitatively the steady-state quenching.
- 7 D. M. Guldi, I. Zilbermann, G. Anderson, A. Li, D. Balbinot, N. Jux, M. Hatzimirinaki, A. Hirsch and M. Prato, *Chem. Commun.*, 2004, 726.
- 8 J. Rodriguez, C. Kirmaier and D. Holton, *J. Am. Chem. Soc.*, 1989, **35**, 6500.
- 9 The Soret-band bleaching tracks nicely the red-shift seen for SWNT-PSS $^{n-}/\text{H}_2\text{P}^{8+}$  relative to  $\text{H}_2\text{P}^{8+}$ .
- 10 The  $\text{H}_2\text{P}^{8+}$   $\pi$ -radical anion, which also exhibits characteristic absorption changes in this spectral range, would be oxygen sensitive.